

# The $A_{Si-Si_i}$ Defect Model of Light-Induced Degradation (LID) in Silicon: A Discussion and Review

Kevin Lauer,\* Katharina Peh, Dirk Schulze, Thomas Ortlepp, Erich Runge, and Stefan Krischok

The  $A_{Si-Si_i}$  defect model as one possible explanation for light-induced degradation (LID) in typically boron-doped silicon solar cells, detectors, and related systems is discussed and reviewed. Starting from the basic experiments which led to the  $A_{Si-Si_i}$  defect model, the  $A_{Si-Si_i}$  defect model (A: boron, or indium) is explained and contrasted to the assumption of a fast-diffusing so-called “boron interstitial.” An LID cycle of illumination and annealing is discussed within the conceptual frame of the  $A_{Si-Si_i}$  defect model. The dependence of the LID defect density on the interstitial oxygen concentration is explained within the  $A_{Si-Si_i}$  defect picture. By comparison of electron paramagnetic resonance data and minority carrier lifetime data related to the assumed fast diffusion of the “boron interstitial” and the annihilation of the fast LID component, respectively, the characteristic EPR signal Si-G28 in boron-doped silicon is related to a specific  $A_{Si-Si_i}$  defect state. Several other LID-related experiments are found to be consistent with an interpretation by an  $A_{Si-Si_i}$  defect.

## 1. Introduction

Light-induced degradation (LID) in boron-doped silicon which is oxygen contaminated during crystal growth is still a problem in silicon technology such as silicon solar cells or radiation detectors. A recent review of Lindroos and Savin on this topic summarizes the work of more than four decades of research.<sup>[1]</sup> Recently, a mitigation procedure for LID was established,<sup>[2]</sup> which introduces a costly separate step in, for example, solar cell production lines. Another more widely used approach to overcome the LID problem in boron-doped silicon is to use gallium-doped silicon

for solar cell production.<sup>[3]</sup> However so far no final, generally adopted solution to the LID problem has been presented.

Due to the impact of LID on solar cell processing, detector processing, and the efficiency, much effort has been and is currently spent on the investigation of the underlying defect. Nevertheless, no consensus was reached regarding the defect composition as well as the defect model. In this contribution, the experimental evidence for an LID scenario, namely, the  $A_{Si-Si_i}$  defect model is critically discussed and reviewed.

## 2. Basic Experiments on Light-Induced Degradation


The idea for the  $A_{Si-Si_i}$  defect model was developed in 2013 after the discovery of LID in indium-doped silicon<sup>[4]</sup>. At that time, indium-doped silicon was investigated with respect to acceptor iron pairs, which are well known. During these investigations,<sup>[5]</sup> it was found that indium-doped silicon shows a similar LID behavior as boron-doped silicon (see **Figure 1**). A fast and a slow LID component are seen in both cases. This basic experimental finding led to a controversial discussion since an earlier investigation<sup>[6]</sup> had not observed LID in indium-doped silicon. We confirmed LID in indium-doped silicon by the investigation of indium-doped samples specifically grown at IKZ in Berlin.<sup>[7,8]</sup> It has to be noted that the LID defect in these samples is most probably generated during the Czochralski silicon crystal growth and cooling process.

After the discovery of LID in indium-doped silicon, several publications looked for LID in solar cells manufactured from indium-doped silicon.<sup>[9–12]</sup> After some negative results, a first indication that LID is indeed present in indium-doped silicon was found by Binns et al.<sup>[11]</sup> They found a small but unquestionable LID in indium-doped silicon: It was observed by charge carrier lifetime measurements on surface-passivated samples. Later on, a fast and reversible degradation in indium-doped surface-passivated silicon wafers was reported by Murphy et al., again using carrier lifetime measurements.<sup>[13]</sup> Recently, LID in indium-doped silicon was convincingly verified by Guzman et al.<sup>[14]</sup> They showed microwave-detected photoconductance decay (MWPCD) lifetime maps before and after illumination and found a strong degradation of the carrier lifetime due to the LID.

In summary, one can state that LID, although being a serious problem in solar cells from boron-doped silicon and observed in

K. Lauer, T. Ortlepp  
CIS Forschungsinstitut für Mikrosensorik GmbH  
Konrad-Zuse-Str. 14, 99099 Erfurt, Germany  
E-mail: kevin.lauer@tu-ilmenau.de

K. Lauer, K. Peh, D. Schulze, E. Runge, S. Krischok  
Institut für Physik und Institut für Mikro- und Nanotechnologien  
TU Ilmenau  
98693 Ilmenau, Germany

 The ORCID identification number(s) for the author(s) of this article can be found under <https://doi.org/10.1002/pssa.202200099>.

© 2022 The Authors. physica status solidi (a) applications and materials science published by Wiley-VCH GmbH. This is an open access article under the terms of the Creative Commons Attribution License, which permits use, distribution and reproduction in any medium, provided the original work is properly cited.

DOI: 10.1002/pssa.202200099

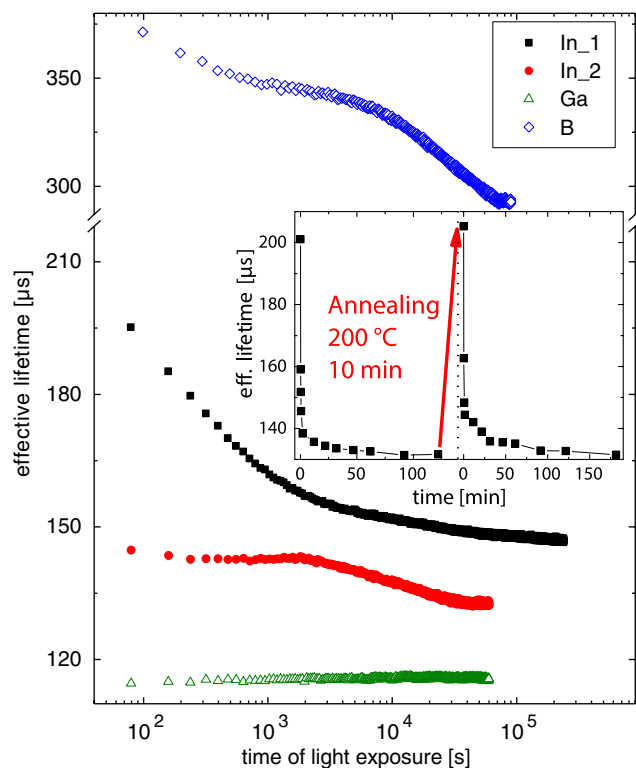


**Figure 1.** Charge carrier lifetime as a function of illumination time for a boron-, a gallium-, and two indium-doped silicon samples. Clearly visible is the LID in boron- and indium-doped silicon but not in gallium-doped silicon. The inset illustrates LID reversal by annealing. Reproduced with permission.<sup>[4]</sup> Copyright 2013, Wiley VCH.

surface-passivated indium-doped silicon wafers, is generally not found in solar cells made from indium-doped silicon. Possibly, the passivation of LID in indium-doped silicon during a solar cell process is easier compared with the boron case. Thereby passivation by hydrogen is the most likely process as discussed later.

Besides the charge carrier lifetime experiments, a second class of experiments exists which we will discuss in detail because they strongly support the  $A_{Si-Si_i}$  defect theory. It is photoluminescence spectroscopy on indium-implanted silicon. In indium-doped silicon, a characteristic photoluminescence line called “P line” was discovered<sup>[15,16]</sup> early but could despite much effort (see references in the study by Lauer et al.<sup>[17]</sup>) not be identified with a defect in silicon. Fortuitously, after publishing LID in indium-doped silicon,<sup>[4]</sup> we got specially prepared indium-implanted samples from the company Infineon Technology AG, which allowed in-depth PL investigations of the P line (see Figure 2).<sup>[17]</sup> Here, we recall three key observations. First, the P line was found in samples, where a silicon interstitial-rich (SIR) region coincides with the peak of the implanted indium profile. The SIR region was generated by carbon coimplantation. At the interface between amorphous and crystalline silicon, an SIR region forms. By varying the carbon implantation energy, the amorphous/crystalline interface and hence the SIR region can be shifted. We found for the group with low-indium dose that the appearance of the P line depends on whether the SIR

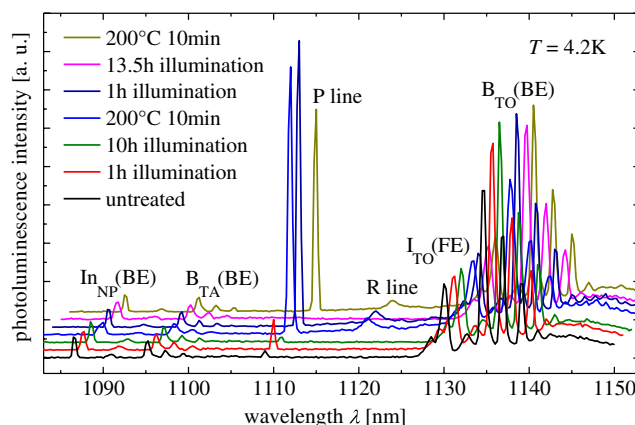


**Figure 2.** Photoluminescence spectra during different steps of LID cycling of an indium-implanted silicon sample. The P line clearly follows the LID cycle. Adapted under the terms of the Attribution 3.0 Unported (CC BY 3.0) license.<sup>[17]</sup> Copyright 2015, the Author(s), Published by AIP Publishing LLC.

region is placed on the indium peak or behind the indium peak. The P line only appears if the SIR region is placed on the indium peak. This key observation suggested that the P line could be caused by a defect involving indium and silicon interstitials. One possible, very plausible, candidate for such a defect is the  $In_{Si}-Si_i$  defect.<sup>[17]</sup> If this is the case, the P line intensity should follow the LID cycle as observed for the carrier lifetime in indium-doped silicon. In fact as the second key observation, the P line follows the LID cycle of illumination and annealing,<sup>[17]</sup> as is clearly seen in Figure 2: The maximum P line intensity appears in the intermediate state after 1 h illumination. The P line disappeared completely after long illumination of about 13 h. The process was reversible by 10 min annealing at 200 °C. This was at that time a quite surprising result and strongly supports the identification of the P line as  $In_{Si}-Si_i$  defect. A detailed interpretation of these results in the framework of the  $A_{Si-Si_i}$  defect model will be given in Section 4.

The third key observation was that a hydrogen-rich silicon nitride layer on top of the silicon leads to a complete disappearance of the P line after the 200 °C annealing step.<sup>[17]</sup> This could be explained by passivation of the  $In_{Si}-Si_i$  defect by hydrogen, which possibly leads to an  $In_{Si}-Si_i-H$  defect.<sup>[18]</sup> A similar passivation of LID in boron-doped silicon was first reported by Herguth et al.<sup>[19]</sup> The finding of a passivation of LID in indium-doped silicon by hydrogen from a silicon nitride layer would also explain why no LID is observed in commercial indium-doped silicon solar cells. This is because in solar cells usually hydrogen-rich layers are used for passivation of the surface recombination.

### 3. The $A_{Si-Si_i}$ Defect Model

Based on the above described experiments, one of the authors proposed the  $A_{Si-Si_i}$  defect to be responsible for LID in boron- and indium-doped silicon.<sup>[4]</sup> The basic idea for this proposal stems from ab initio simulations of defects, where one acceptor atom and one silicon atom share a lattice position in silicon.<sup>[20–23]</sup> These simulations showed a striking difference between the

acceptors boron and indium on the one hand and gallium on the other hand. In these simulations, the formation energy of different configurations of this kind of defect was calculated. For the case of boron and indium doping, the lowest formation energy was found for the configuration where the acceptor stays near the substitutional position and the silicon resides on an interstitial position (see **Figure 3**). Hence, this kind of defect was named  $A_{Si}-Si_i$  defects. For gallium doping, the lowest energy configuration is found if gallium leaves the substitutional position and resides on a tetrahedral interstitial position.

In addition, it was found that the charge state of the defect has an impact on the microscopic configuration of the  $B_{Si}-Si_i$  defect. Hakala et al.<sup>[20]</sup> found that the +1 charge state of the  $B_{Si}-Si_i$  defect has  $C_{3v}$  symmetry, whereas the neutral and -1 charge can exist in the  $C_{3v}$  or  $C_{1h}$  symmetry. For their interpretation, it seems worthwhile to look at the configurations of a silicon interstitial in silicon. Jones et al.<sup>[24]</sup> simulated three possible positions of a silicon interstitial in silicon. One is the split interstitial (*D*) configuration, where two silicon atoms share one lattice position. Another one is the hexagonal position (*H*), where the silicon interstitial resides in the middle of a ring of six lattice atoms. The third one is the tetrahedral position (*T*), where the interstitial silicon sits in the middle of the triangular pyramid formed by lattice atoms. Jones et al. also calculated the energy barriers in between the three configurations. They plotted a configuration coordinate energy diagram for the case of n-type silicon. From this diagram, we deduced a configuration coordinate energy diagram for the  $A_{Si}-Si_i$  defect in p-type silicon: It is illustrated schematically in **Figure 4** and involves three configurations  $S_1$ ,  $S_2$ , and  $S_3$ , with the three possible charge states '+', 'neutral,' and '-'.<sup>[8]</sup> Further, we assumed that the main changes in the  $A_{Si}-Si_i$  defect during illumination and annealing steps are due to configuration changes of the silicon interstitial itself.

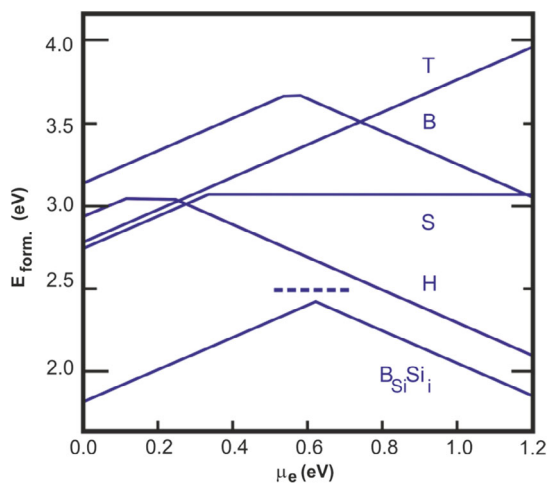


**Figure 3.** Formation energies for interstitial B configurations as a function of the position of the Fermi level ( $\mu_e$ ), after the study by Hakala et al.<sup>[20]</sup> The  $B_{Si}-Si_i$  defect has the lowest formation energy compared with the other interstitial positions *T*, *B*, *S*, and *H*, as discussed in studies by Hakala and Jones et al. in refs. [20] and [24]. Adapted (Figure 2) with permission.<sup>[20]</sup> Copyright 2000, American Physical Society.

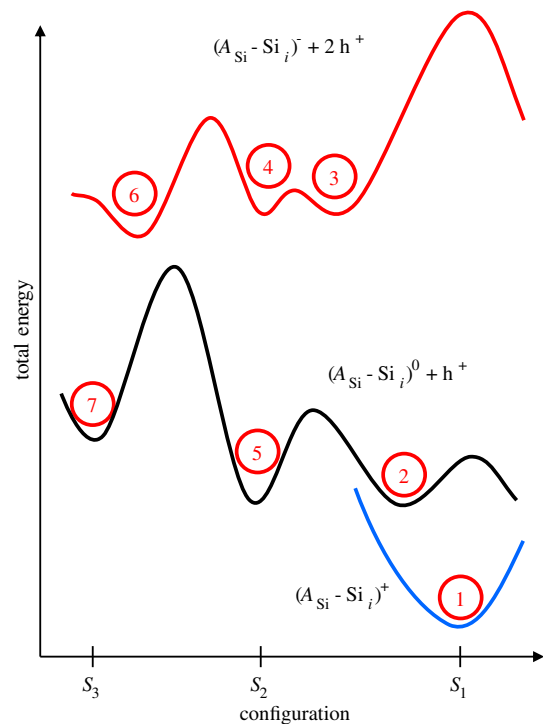


**Figure 4.** Configuration coordinate energy diagram proposed for the  $A_{Si}-Si_i$  defect in p-type silicon. Possible states of the  $A_{Si}-Si_i$  defect configurations  $S_1$ ,  $S_2$ , and  $S_3$  are numbered from 1 to 7, see text. Adapted with permission.<sup>[8]</sup> Copyright 2017, Wiley-VCH.

#### 4. Explanation of the LID Cycle by the $A_{Si}-Si_i$ Defect Model

The density functional theory (DFT) data from literature<sup>[24]</sup> suggest to identify the different configurations  $S_1$ ,  $S_2$ , and  $S_3$  with the *T*, *H*, and *D* configurations, respectively, but further work to confirm the interpretation is desirable. The observed LID cycle is now explained by configuration changes of seven possible states of the  $A_{Si}-Si_i$  defect, which are actuated by thermal energy after charge state changes.<sup>[8]</sup> Note that different charge states of the same defect as illustrated in Figure 4 lead to slightly different ion positions (indicated by lateral displacements on the symbolic configuration axis in Figure 4) and as a consequence to different energy barriers for transitions between configurations. The ground state, which is, for example, in the experiment of Figure 1, reached after the 200 °C annealing step, is called state 1. During illumination, two holes are emitted or two electrons are captured by the  $A_{Si}-Si_i$  defect, most likely sequentially via state 2, and state 3 is reached. The thermally driven transition from state 3 to 4 is the fast step in the LID process that can be seen, for example, in Figure 1. It is visible in the carrier lifetime as the Shockley–Read–Hall<sup>[25,26]</sup> (SRH) parameters in configuration  $S_2$  are in this model sufficiently different from those of configuration  $S_1$ . Obviously, from state 3 to state 4, an energy barrier  $E_{34}$  must be surmounted. If the illumination stops here, which is 1 h for typical solar cell conditions, then a hole is captured and the  $A_{Si}-Si_i$  defect falls into state 5. The transition from state 5 to state

2 and finally state 1 is referred to hereafter as the annihilation of the fast LID component.

The slow component of LID, which is identified as the transition from state 4 to state 6, has a higher-energy barrier  $E_{46}$ . Hence, the process is slower at any given temperature than the transition from state 3 to 4. In configuration  $S_3$ , a transition from state 6 to 7 takes place while a hole is captured. The SRH parameters are again different from those of  $S_2$  and hence the transition 4 to 6 becomes visible in the carrier lifetime as well. If now the illumination or carrier injection is turned off, a hole is captured again and the  $A_{Si-Si_i}$  defect stays in configuration  $S_3$  as the barrier  $E_{75}$  is too high to be surmounted at, for example, room temperature. Only if the temperature is raised to about 200 °C or more for several minutes, enough thermal energy for crossing the barrier  $E_{75}$  is available and state 1 can be reached again and the LID cycle is closed.

One important point which is not discussed so far is that the transitions of the defect must be considered as equilibrium reactions.<sup>[8]</sup> This means that, for example, during the slow component of LID (transition 4 to 6) the backward transition (6 to 4) takes place. Finally, an equilibrium will form where still some defects are in state 4. If now a short dark anneal is applied those defects, which were still in state 4, while illumination, they are transferred into their ground state 1. Under following illumination in the extreme case of a very short dark anneal, only a fast LID component would be visible in the carrier lifetime measurements. During the short dark anneal, only a very small number of defects in state 7 are able to surmount the barrier  $E_{7,5}$ . Depending on the duration of the short dark anneal, more of the slow LID component would become visible. This behavior was recently impressively demonstrated by Kim et al.<sup>[27]</sup> and also by Schmidt et al.<sup>[28]</sup> One should expect significant remaining defect activity after a short dark anneal. Not much has been published on this subject, but the lifetimes reported in the study by Schmidt et al.<sup>[28]</sup> support this expectation.

After the interpretation of a typical LID cycle observed in boron- and indium-doped silicon in terms of the  $A_{Si-Si_i}$  defect model, we turn to the behavior of the  $P$  line during the LID cycle and its explanation in frame of the  $A_{Si-Si_i}$  defect model: The maximum intensity of the  $P$  line is observed after annealing at 200 °C for 10 min and 1 h illumination (see Figure 2). Therefore, we identify state 5 in configuration  $S_2$  with the defect state responsible for the  $P$  line. It is the neutral  $In_{Si-Si_i}$  defect in configuration  $S_2$  which binds the exciton. This bound exciton recombines and the characteristic photon for the sharp  $P$  line is emitted. With this identification, the changes in the  $P$  line during an LID cycle can be easily explained by the  $A_{Si-Si_i}$  defect model: After long illumination, the  $P$  line disappears as the defect is in configuration  $S_3$ , which has different recombination parameters and is assumed to be not active in photoluminescence. The annealing step transfers most  $A_{Si-Si_i}$  defects into state 1. As a consequence, the  $P$  line should also not be visible after the 200 °C for the 10 min annealing step. We attribute the fact that it is still visible, to experimental circumstances. We had to illuminate with the PL excitation laser for a long time (>30 min) at low temperature ( $T < 20$  K) to measure the spectra and, most likely, inadvertently populated state 5 of the  $In_{Si-Si_i}$  defect.<sup>[17]</sup>

Unfortunately, we had no information about the status of the sample without any intentional treatment (untreated) with respect to the LID cycle. It seems natural to assume a mix of

defect states 1, 5, and 7, with the majority of defects being in state 7. Hence, we find the  $P$  line in the untreated case caused by state 5 and the transition of some defects from state 1 to 5 during measurement. During short illumination we find an increase in  $P$  line since most of the defects are transferred from state 1 to state 5 now. Further illumination causes the transition from state 4 to 6 and finally to state 7, which leads to a decrease in the  $P$  line.

It is clear that the barrier between state 3 and 4 cannot be surmounted thermally at such low temperatures as necessary for low-temperature photoluminescence spectroscopy. Hence, we suspect a recombination-enhanced defect reaction (REDR) mechanism<sup>[29]</sup> to provide the necessary energy. Experimental support for the idea that state 5 is populated at low temperatures by illumination comes from the EPR results discussed in Section 5.2 in this contribution. The EPR signal SiG28 becomes visible at low temperatures only after illumination. Carefully designed experiments which are underway are necessary to clarify the behavior of the  $P$  line in particular after the dark anneal.

## 5. Discussion of the $A_{Si-Si_i}$ Defect Model

The publication of the  $A_{Si-Si_i}$  defect model led to a vivid discussion since it seemed to be incompatible with former experimental data<sup>[30,31]</sup> or, to be precise, with the generally accepted interpretation thereof. However, a closer look reveals that the  $A_{Si-Si_i}$  defect model is consistent with the existing experimental data from other groups but simply provides a slightly different interpretation thereof.<sup>[18]</sup> The main results to be interpreted and their explanation within the  $A_{Si-Si_i}$  defect are briefly reviewed next.

### 5.1. Role of Oxygen

Early work found an approximately quadratic dependence of the LID defect concentration on the interstitial oxygen concentration.<sup>[30]</sup> Naturally, this led to several defect models which include an oxygen dimer within the defect: First a  $B_{Si-O_2}$  defect was suggested where the LID defect cycle was explained by the association and dissociation of the dimer from the substitutional boron assuming fast diffusion of the oxygen dimer.<sup>[30]</sup> Most recently, the formation of an  $A_{Si-O_2}$  defect was proposed,<sup>[32]</sup> where the LID defect cycle was explained by a charge state change-induced configuration change similar to the  $A_{Si-Si_i}$  defect model. The fundamental difference between the two recent defect models is the incorporation of either a silicon interstitial or an oxygen dimer in the defect.

The argument that a dependence on the oxygen availability implies oxygen-containing defects is less stringent than it appears at first sight. On the one hand, no in-depth explanation is given in the literature so far as to why quadratic dependency of the LID defect concentration implies an oxygen dimer incorporation in the defect. On the other hand, there is at least one efficient mechanism on how the presence of oxygen leads to silicon interstitials:<sup>[18]</sup> If the interstitial oxygen concentration in silicon is above the solubility limit and the temperature is high enough for oxygen diffusion, oxygen tends to form clusters. Theoretically, for two clustering interstitial oxygen atoms, one silicon interstitial is ejected as the  $SiO_2$  phase needs more space than the two interstitial oxygen atoms themselves.<sup>[33]</sup> This naturally would explain a quadratic dependency of the Si



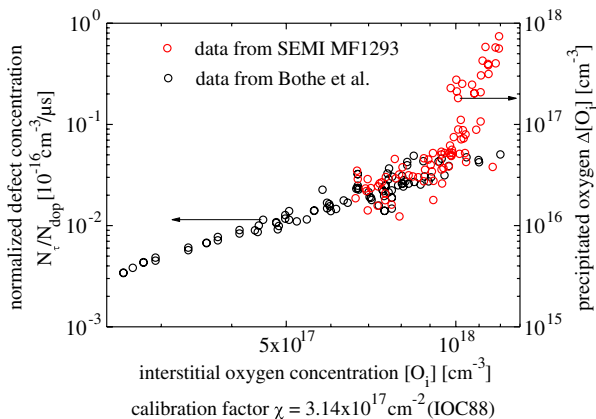


**Figure 5.** Comparison of normalized LID defect concentration<sup>[30]</sup> and precipitated oxygen concentration after annealing steps<sup>[37,38]</sup> as a function of interstitial oxygen concentration (see text).

interstitial concentration on the interstitial oxygen concentration. A theoretical description is given by Tan and Taylor.<sup>[34]</sup> Simulations done by Kissinger et al.<sup>[35]</sup> show also that for small oxygen nuclei, which form during CZ crystal cooling below 1000 °C, the factor for the number of emitted silicon interstitial atoms divided by the number of precipitated oxygen atoms is about 0.5.

Experimentally, some oxygen-clustering experiments show that the clustered oxygen concentration depends quadratically on the interstitial oxygen concentration,<sup>[18]</sup> which could imply roughly quadratic increase of the silicon interstitials. Also, the scatter in the data, which is observed in the experimental data of the LID defect concentration, fits well to the oxygen-clustering data (see **Figure 5**). The strong scatter in the data, which is observed in the range from 6 to  $10 \times 10^{17} \text{ cm}^{-3}$ , is a strong indication that oxygen is not directly, but rather indirectly, involved in the defect responsible for LID.<sup>[36]</sup> It has to be noted that the precipitated oxygen fraction as a function of the initial interstitial oxygen concentration depends on the applied thermal processes.<sup>[35]</sup> A comparison of the CZ crystal growth and cooling process with an annealing at 1050 °C for 16 h, as done in **Figure 5**, must hence be taken with caution and can be used only

as first approximation. A comparison of the LID density and the precipitated oxygen concentration for samples which were treated similarly would be extremely desirable. The ejected silicon interstitial forms then, besides other reactions, the  $\text{A}_{\text{Si}}\text{-Si}_i$  defect. We will discuss in Section 5.2 that for the cases of boron and indium doping, the so-called “Watkins replacement reaction”, where the substitutional acceptor atom is kicked out to an interstitial position, most likely does not take place.

The explanation of  $\text{Si}_i$  resulting from oxygen clusters suggests a more or less homogenous distribution of oxygen clusters in the as-grown Czochralski silicon crystal. However, in Czochralski silicon crystals, the observed bulk microdefects (BMD) can show depending on the growth process a pronounced pattern,<sup>[39,40]</sup> which is explained by the Voronkov model.<sup>[41,42]</sup> This pronounced BMD pattern, see in particular the line scans of **Figure 6d** of the study by Hourai et al.,<sup>[40]</sup> is linked to vacancy or silicon interstitial-rich regions in the crystal. In an experiment related to these regions, no impact of this pattern on the LID could be found.<sup>[43]</sup> Unfortunately, the usually applied methods to measure the BMD density have a low detection efficiency<sup>[44–46]</sup> and typically only about 10% of the existent BMDs become visible, that is, 90% of the oxygen clusters remain invisible.<sup>[45]</sup> It should also be noted that in nitrogen-doped CZ silicon crystals the discrepancy between the concentrations of visible and invisible oxygen clusters is much smaller.<sup>[45]</sup> In addition, the BMD measurement is typically made after oxygen precipitate growth treatments like two-step annealing at, for example, 800 and 1000 °C for several hours. Hence the BMD measurements represent mainly the oxygen precipitates which grow under those special conditions. They do not represent the small oxygen nuclei formed during crystal cooling below 1000 °C, which are thought to be responsible for the silicon interstitial emission needed for the  $\text{A}_{\text{Si}}\text{-Si}_i$  defect formation. These small oxygen nuclei are distributed homogeneously irrespective of the crystal-growing regime.<sup>[47]</sup> Therefore, the  $\text{A}_{\text{Si}}\text{-Si}_i$  defect model can neither be rejected based on the actual measurements of the BMD density nor by the downstream theories<sup>[41,42]</sup> which explain the BMD patterns.

It should be noted that the creation of LID was found in diffusion-oxygenated FZ (DOFZ) silicon wafers treated at 650 °C.<sup>[50]</sup> Obviously, further carefully designed experiments are necessary which include the solar cell fabrication process

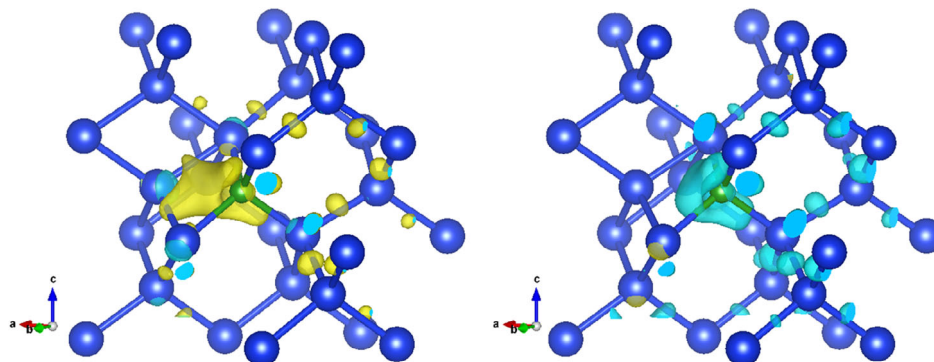


**Figure 6.** Illustration of the  $\text{B}_{\text{Si}}\text{-Si}_i$  defect in the  $\text{S}_1$  (T) configuration indicating the distribution of an extra hole (left) and an extra electron (right), obtained within the LDA approximation using the VASP code,<sup>[48]</sup> illustrated using the VESTA software.<sup>[49]</sup> Different charge states of the defect are accompanied by minor local adjustments of the ion positions.

or layer deposition processes to finally prove the impact of silicon self-interstitials on the LID. At present, an  $A_{Si-Si_i}$  defect can neither be ruled out, nor be proven by existing experimental data.

## 5.2. “Boron Interstitial” Investigated by EPR

Another widely held belief which seemingly contradicts the  $A_{Si-Si_i}$  defect model is the high mobility of the so-called “boron interstitial”  $B_i$ .<sup>[51]</sup> As early as 1975, Watkins<sup>[31]</sup> proposed three models for extra boron in the silicon lattice. In all three models, boron has left its substitutional place and yields a highly mobile defect. From today’s perspective, one has to state that all three models are most probably wrong since all ab initio simulations find the lowest formation energy for configurations with boron staying near a substitutional place.<sup>[20,52–56]</sup> The fact that the recent DFT results contradict the established, almost half-a-century-old interpretations of early experiments called for new experiments. Thus, a group around one of the authors had a close look on experimental data related to LID and the so-called “boron interstitial”.<sup>[17]</sup> The most relevant result is shown in Figure 7. The neutral “boron interstitial” was found to be strongly correlated to a Si-related electron paramagnetic resonance (EPR) signal called Si-G28.<sup>[31]</sup> This signal appeared in boron-doped silicon after electron irradiation and most importantly after subsequent illumination with near-bandgap light. It started to disappear again after warming to, for example, 50 K in the dark. The disappearance rate of this EPR signal as a function of the inverse temperature is replotted in Figure 7. In addition, the annihilation of the fast LID component, which was measured by the change in the open-circuit voltage ( $V_{OC}$ ) of solar cells,<sup>[30]</sup> is included in Figure 7 as well. Within the frame of the  $A_{Si-Si_i}$  defect model, the annihilation of the fast LID component is identified with the transition from state 5 to

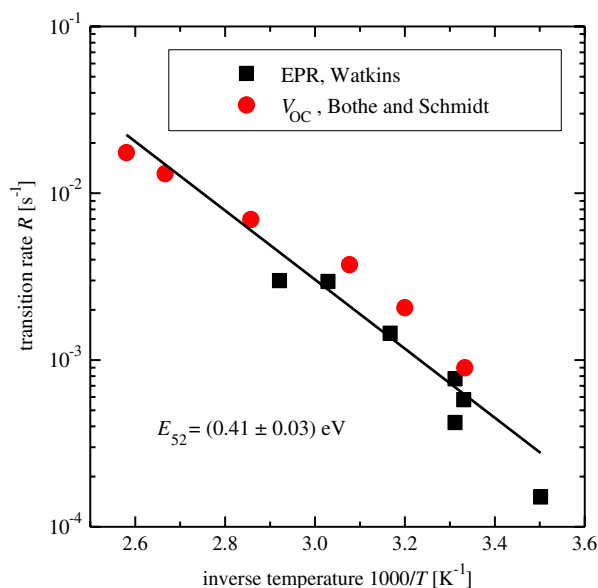


**Figure 7.** Transition rate of transition from state 5 to state 2 in the  $A_{Si-Si_i}$  defect model as a function of inverse temperature: EPR data<sup>[31]</sup> (black squares) are compared with  $V_{OC}$  data (open-circuit voltage of solar cells)<sup>[30]</sup> (red dots, adapted under the terms of the Attribution 3.0 Unported (CC BY 3.0) license.<sup>[17]</sup> Copyright 2015, the Author(s), Published by AIP Publishing LLC).

state 1. The energy barrier  $E_{52}$  must be crossed for transition from state 5 to state 2 and a hole must be captured to reach state 1 from state 2. As shown in Figure 7, the experimental data of the transition rate related to the annihilation of the fast LID component and the disappearance of the light-induced EPR signal in boron-doped silicon agree extremely well. Hence, we conclude that the measured EPR signal Si-G28 in boron-doped silicon most likely stems from the  $B_{Si-Si_i}$  defect in state 5. The observed appearance and disappearance of the EPR signal by illumination and annealing, respectively, can hence be explained by charge state change-induced configuration changes in the  $A_{Si-Si_i}$  defect model. The old assumption of extremely fast diffusion of boron is in this case no longer necessary.

## 5.3. “Boron Interstitial” Investigated by Other Methods

Next, we review other experiments besides EPR which have been addressed in the discussion of on the one hand the  $A_{Si-Si_i}$  defect model and on the other hand the concept of fast diffusion of the postulated “boron interstitial”. These are deep-level transient spectroscopy (DLTS),<sup>[57–59]</sup> infrared (IR) absorption spectroscopy,<sup>[60]</sup> channeling experiments,<sup>[61,62]</sup>  $\beta$ -radiation-detected nuclear magnetic resonance ( $\beta$ -NMR),<sup>[63,64]</sup> and secondary-ion mass spectrometry (SIMS).<sup>[65]</sup> A common problem of these methods (except SIMS) is that they cannot distinguish whether the disappearance of a signal is due to motion of atoms or due to a reconfiguration of a defect.

In a series of DLTS experiments,<sup>[57–59]</sup> the Watkins group investigated the “boron interstitial”. They found two DLTS signals  $E(0.45)$  and  $E(0.23)$  in electron-irradiated boron and phosphorous-doped n-type silicon.<sup>[57]</sup> It should be mentioned that LID is observed not only in boron-doped p-type silicon but also in boron-compensated n-type silicon as well.<sup>[66]</sup> The Watkins group attributed the first level to the “boron interstitial” defect. The latter DLTS level was for a while identified by the community as a defect consisting of  $B_i$  and  $O_i$ ,<sup>[51]</sup> but after a careful experiment of Lasse Vines et al.,<sup>[67]</sup> the  $E(0.23)$  level should now be treated as unidentified. The Watkins group found that the disappearance of  $E(0.45)$  coincides with the appearance of the  $E(0.23)$  level and that the  $E(0.45)$  level could only be seen in n-type and not in p-type silicon. They also found that the disappearance rate of the  $E(0.45)$  level is enhanced by minority carrier injection. In the second paper of that series,<sup>[58]</sup> a third DLTS signal  $E(0.13)$  is found, which is activated by illumination. The last paper in the series<sup>[59]</sup> is the most relevant one in the present context because it reopens the discussion of the nature of the defect and now questions the hypothesis of migration of the “boron interstitial” by the Bourgoin–Corbett mechanism which was assumed so far. The authors tried to induce the migration of “interstitial boron” by experimentally cycling between different states of the “boron interstitial” and found no disappearance of the original signal. This shows that cycling is fully reversible and that no trapping after eventual migration occurs. This fits well to the observations of the LID cycle, which is also completely reversible.

We turn to absorption spectroscopy and in particular to an experiment by Tipping and Newman,<sup>[60]</sup> who found two IR absorption lines  $^{10}R$  and  $^{11}R$  which they identify with “interstitial boron”. The identification was made by the frequency ratio of absorption lines resulting from  $^{10}B_s$  and  $^{11}B_s$ . The R lines were

found to anneal out and new lines denoted by *S* and *Q* appeared. If the annealing of the *R* lines was evaluated assuming first-order kinetics, an activation energy  $E_A = 0.43$  eV was found. This is in good agreement with the activation energy we found for the transition from state 5 to 2 (s. Figure 7). It is possible that the IR absorption line *R* is related to state 5 in the  $A_{Si-Si_i}$  defect model. The *S* and *Q* IR absorption lines could be identified with state 2 and 1, respectively. Hence, the reported experimental IR absorption spectroscopy data do not contradict the  $A_{Si-Si_i}$  defect model, they rather support it.

Another method to investigate the lattice position and the amount of the “boron interstitial” defect is the channeling technique.<sup>[61,62]</sup> North and Gibson<sup>[62]</sup> reported that after room-temperature implantation  $\approx 70\%$  of the boron was on an interstitial position. The amount of boron residing in interstitial position increases under annealing slightly up to  $\approx 800$  °C and then rapidly disappears. These measurements neither support nor contradict the  $A_{Si-Si_i}$  defect model. It is probable that after room-temperature implantation of boron most of the boron forms the  $B_{Si-Si_i}$  defect in configuration  $S_3$ , since the boron implantation generates a lot of charge carriers. More charge carriers are generated during the channeling measurement by the proton beam and hence the  $B_{Si-Si_i}$  defect stays in configuration  $S_3$ . The decrease of the interstitial component above 800 °C could be explained by dissociation of the  $B_{Si-Si_i}$  defect. It should be mentioned that these channeling studies contradict the idea of Watkins that “interstitial boron” is highly mobile and is trapped by other defects even below room temperature since an “interstitial boron” signal is detected up to 800 °C.

The next experiment which will be briefly discussed here is the  $\beta$ -NMR experiment by Seelinger et al.<sup>[63]</sup> on samples where  $^{12}B$  atoms were implanted at varying temperatures. Results on the lattice location of “interstitial boron” and on the amount of substitutional boron as a function of implantation temperature are reported. The conclusions are similar to the channeling experiments: The “boron interstitial” is not in a tetrahedral configuration and boron becomes more and more substitutional by increasing the temperature. Again, these results neither contradict nor support the idea of an  $A_{Si-Si_i}$  defect model.

Finally, it should be noted that SIMS experiments<sup>[65]</sup> indeed found hints of boron migration at room temperature, however only under large silicon interstitial injection as it occurs during sputtering for SIMS analysis<sup>[68]</sup> and for high-concentration gradients. These conditions are not at all met by the situation

which is prevalent in the case of the vanishing light-induced Si-G28-EPR signal observed by Watkins. Hence, these SIMS experiments are no direct proof that the “boron interstitial” is indeed moving fast under the conditions applied for the EPR investigations.<sup>[31]</sup> It is possible that the  $B_{Si-Si_i}$  defect is the mobile species of boron at higher temperatures as discussed for the diffusion process<sup>[69]</sup> and that the signal changes related to the “interstitial boron” around room temperature are due to configuration changes of the  $B_{Si-Si_i}$  defect.

Despite the support of the  $A_{Si-Si_i}$  defect model by existing experimental data related to the “boron interstitial” and by the oxygen nucleation experiment and theory, further experimental and theoretical testing of the  $A_{Si-Si_i}$  defect model is necessary. At present, DFT simulations and measurements of the energy barriers  $E_{xy}$ , with *x* and *y* being neighboring states of the  $A_{Si-Si_i}$  defect model (see Figure 4), are initiated. If the numerically obtained and the measured energy barriers coincide, this would be a further strong hint for the correctness of the  $A_{Si-Si_i}$  defect model.

First simulation results are depicted in Figure 6. They show the distribution of the extra hole (left) for  $B_{Si-Si_i}^+$  and the extra electron (right) for the  $B_{Si-Si_i}^-$  in configuration  $S_1$  (*T*), respectively.

In Table 1 the main experimental results and their explanation within the  $A_{Si-Si_i}$  defect model discussed in Section 5 are summarized.

## 6. Summary and Outlook

LID is a problem for CZ silicon solar cells. It appears in boron- and indium-doped silicon and reduces considerably the charge carrier lifetime and, in particular in boron-doped silicon, the solar cell efficiency. Despite more than 40 years of research on the defect responsible for LID, no consensus has been reached regarding defect composition and defect model. In a series of experiments and publications, we put forward the  $A_{Si-Si_i}$  defect model to explain and model the reported LID properties. This model and possible counter arguments as well as ramifications of the  $A_{Si-Si_i}$  defect model on the interpretation of published data were discussed and reviewed in this contribution.

We started from the experiments which led to the idea of the  $A_{Si-Si_i}$  defect model, namely, the observation of LID in indium-doped silicon and the correlation of LID with the so-called P line. The model is described and a complete LID cycle of light

**Table 1.** Main experimental results which are discussed in Section 5 with its explanation within the  $A_{Si-Si_i}$  defect model.

Experimental results	Explanation within $A_{Si-Si_i}$ defect model
Quadratic dependency of LID density on $O_i^2$	Oxygen clustering during CZ crystal growth and cooling with interstitial ejection (Section 5.1)
No impact of $Si_i$ or V-rich regions detected by BMD on LID density	BMD density does not represent small oxygen nuclei, which form during crystal cooling (Section 5.1)
Light-induced EPR signal SiG28	$B_{Si-Si_i}$ in state 5, annihilation rate of SiG28, and fast LID component coincide (Section 5.2)
Disappearance of $B_i$ observed by infrared absorption spectroscopy	Observed activation energy coincides with annihilation of the fast LID component (process $5 \Rightarrow 1$ ) (Section 5.3)
Annealing of DLTS peaks in boron-compensated n-type silicon	Open question, since LID model for n-type silicon is lacking (Section 5.3)
$B_i$ not at tetrahedral position observed by channeling technique	B remains near substitutional place in the $A_{Si-Si_i}$ defect model (Section 5.3)

absorption, degradation, and annealing is explained in frame of the  $A_{Si-Si_i}$  defect model.

The  $A_{Si-Si_i}$  defect model has strong implications on the understanding of oxygen nucleation in CZ silicon and on the understanding of the “boron interstitial” defect with its downstream-assumed defect reactions. Careful reexamination of experimental data regarding oxygen nucleation and EPR data of the “boron interstitial” defect shows that the experimental data are not in contradiction to the  $A_{Si-Si_i}$  defect model; some data even support the  $A_{Si-Si_i}$  defect model. In addition, other methods which are used to investigate the “boron interstitial” are discussed and it is found that it is not possible to rule out the  $A_{Si-Si_i}$  defect model by these methods.

The observed quadratic dependency of the LID defect density on the interstitial oxygen concentration could be seen as an argument against the  $A_{Si-Si_i}$  model but is explained theoretically and experimentally by oxygen nucleation and silicon interstitial generation. Another concept possibly contradicting the  $A_{Si-Si_i}$  defect model is the notion of a highly mobile “boron interstitial” defect. That picture interprets the disappearance of an EPR signal ( $Si-G28$ ), which was generated by illumination, due to the movement of  $B_i$  to another sink such as, for example,  $O_i$ . However, this implies an extremely fast and hence unlikely diffusion of boron toward these sinks. We showed that the underlying experimental data, which is the disappearance rate of the EPR signal as a function of inverse temperature, coincides with reported experimental data of the annihilation of the fast LID component. Hence, these EPR data can be interpreted as caused by a defect configuration change of the  $B_{Si-Si_i}$  defect from state 5 to state 1. It should be mentioned that defect reactions related to the “boron interstitial” such as, for example, the formation of the so-called “interstitial boron–interstitial oxygen” defect  $B_iO_i$ <sup>[51]</sup> may be an erroneous and premature interpretation of the experimental data.<sup>[67]</sup> This misinterpretation may be also the reason for the difficulties to understand the recently observed acceptor removal in low-gain avalanche detectors (LGAD).<sup>[70]</sup>

Despite the good fit of existing experimental data related to the presumed “boron interstitial” and the oxygen nucleation to the  $A_{Si-Si_i}$  defect model, further experimental and theoretical support of the  $A_{Si-Si_i}$  defect model idea is necessary. Obviously, quantitative values for the energy barriers  $E_{xy}$ , with  $x$  and  $y$  being neighboring states of the  $A_{Si-Si_i}$  defect model, see Figure 4, are highly desirable. This refers to on the one hand DFT- and nudged elastic band (NEB)<sup>[71]</sup>-based theoretical values for the energy barriers between the different configurations at different charge states and on the other hand to energy barriers derived from the temperature-dependent rates observed during LID cycle measurements. Both routes are currently pursued in our labs. It would be an extremely strong support for the correctness of the  $A_{Si-Si_i}$  defect model if the experimental and theoretical values for the relevant energy barriers would agree.

## Acknowledgements

This work was supported by the projects SimASiSii and PAK 981/1 of the Deutsche Forschungsgemeinschaft (DFG KR 2228/11-1, LA 4623/1-1, RU 1383/6-1, RU 1383/8-1) and the project DELGAD of the BMWi (49MF190042). Karsten Bothe is acknowledged for providing part of the data points in Figure 5.

Open Access funding enabled and organized by Projekt DEAL.

## Conflict of Interest

The authors declare no conflict of interest.

## Keywords

$A_{Si-Si_i}$  defect models, light-induced degradation, silicon

Received: February 17, 2022

Revised: June 27, 2022

Published online: August 16, 2022

- [1] J. Lindroos, H. Savin, *Sol. Energy Mater. Sol. Cells* **2016**, 147, 115.
- [2] B. Hallam, A. Herguth, P. Hamer, N. Nampalli, S. Wilking, M. Abbott, S. Wenham, G. Hahn, *Appl. Sci.* **2017**, 8, 10.
- [3] N. E. Grant, P. P. Altermatt, T. Niewelt, R. Post, W. Kwapil, M. C. Schubert, J. D. Murphy, *Sol. RRL* **2021**, 5, 2000754.
- [4] C. Möller, K. Lauer, *Phys. Status Solidi RRL* **2013**, 7, 461.
- [5] K. Lauer, C. Möller, D. Debbih, M. Auge, D. Schulze, *Solid State Phenom.* **2015**, 242, 230.
- [6] J. Schmidt, K. Bothe, *Phys. Rev. B* **2004**, 69, 024107.
- [7] C. Möller, K. Lauer, *Energy Procedia* **2014**, 55, 559.
- [8] K. Lauer, C. Möller, C. Tessmann, D. Schulze, N. V. Abrosimov, *Phys. Status Solidi C* **2017**, 14, 1600033.
- [9] E. Cho, J.-H. Lai, Y. Ok, A. D. Upadhyaya, A. Rohatgi, M. J. Binns, J. Appel, J. Guo, H. Fang, E. A. Good, in *Photovoltaic Specialist Conf. (PVSC), 2015 IEEE 42nd*, IEEE, Piscataway, NJ **2015**, pp. 1–4.
- [10] E. Cho, Y.-W. Ok, A. D. Upadhyaya, M. J. Binns, J. Appel, J. Guo, A. Rohatgi, *IEEE J. Photovoltaics* **2016**, 6, 795.
- [11] M. J. Binns, J. Appel, J. Guo, H. Hieslmair, J. Chen, T. N. Swaminathan, E. A. Good, in *Photovoltaic Specialist Conf. (PVSC), 2015 IEEE 42nd*, IEEE, Piscataway, NJ **2015**, pp. 1–6.
- [12] N. Balaji, V. Shanmugam, S. Raj, J. M. Y. Ali, M. L. O. Aguilar, I. J. Garcia, J. Rodriguez, A. Aberle, S. Duttgupta, *Sol. RRL* **2019**, 3, 1900027.
- [13] J. D. Murphy, A. I. Pointon, N. E. Grant, V. A. Shah, M. Myronov, V. V. Voronkov, R. J. Falster, *Prog. Photovoltaics Res. Appl.* **2019**, 27, 844.
- [14] J. A. T. De Guzman, V. P. Markevich, I. D. Hawkins, H. M. Ayedh, J. Coutinho, J. Binns, R. Falster, N. V. Abrosimov, I. F. Crowe, M. P. Halsall, A. R. Peaker, *Phys. Status Solidi A* **2021**, 218, 2100108.
- [15] M. A. Vouk, E. C. Lightowers, *J. Lumin.* **1977**, 15, 357.
- [16] G. S. Mitchard, S. A. Lyon, K. R. Elliott, T. C. McGill, *Solid State Commun.* **1979**, 29, 425.
- [17] K. Lauer, C. Möller, D. Schulze, C. Ahrens, *AIP Adv.* **2015**, 5, 017101.
- [18] K. Lauer, C. Möller, D. Schulze, C. Ahrens, J. Vanhellefont, *Solid State Phenom.* **2015**, 242, 90.
- [19] A. Herguth, G. Schubert, M. Kaes, G. Hahn, *Prog. Photovoltaics Res. Appl.* **2008**, 16, 135.
- [20] M. Hakala, M. J. Puska, R. M. Nieminen, *Phys. Rev. B* **2000**, 61, 8155.
- [21] P. Alippi, A. La Magna, S. Scalese, V. Privitera, *Phys. Rev. B* **2004**, 69, 085213.
- [22] C. Melis, G. M. Lopez, V. Fiorentini, *Appl. Phys. Lett.* **2004**, 85, 4902.
- [23] P. Schirra, G. Lopez, V. Fiorentini, *Phys. Rev. B* **2004**, 70, 241101.
- [24] R. Jones, A. Carvalho, J. P. Goss, P. R. Briddon, *Mater. Sci. Eng., B* **2009**, 159–160, 112.
- [25] W. Shockley, W. T. Read, *Phys. Rev.* **1952**, 87, 835.
- [26] R. N. Hall, *Phys. Rev.* **1952**, 87, 387.
- [27] M. Kim, M. Abbott, N. Nampalli, S. Wenham, B. Stefani, B. Hallam, *J. Appl. Phys.* **2017**, 121, 053106.
- [28] J. Schmidt, K. Bothe, V. V. Voronkov, R. Falster, *Phys. Status Solidi B* **2020**, 257, 1900167.
- [29] J. D. Weeks, J. C. Tully, L. C. Kimerling, *Phys. Rev. B* **1975**, 12, 3286.



- [30] K. Bothe, J. Schmidt, *J. Appl. Phys.* **2006**, 99, 013701.
- [31] G. D. Watkins, *Phys. Rev. B* **1975**, 12, 5824.
- [32] M. Vaqueiro-Contreras, V. P. Markevich, J. Coutinho, P. Santos, I. F. Crowe, M. P. Halsall, I. Hawkins, S. B. Lastovskii, L. I. Murin, A. R. Peaker, *J. Appl. Phys.* **2019**, 125, 185704.
- [33] U. Gösele, T. Y. Tan, *Appl. Phys. A* **1982**, 28, 79.
- [34] F. Shimura, *Oxygen in Silicon*, Academic Press, San Diego, California, USA **1994**.
- [35] G. Kissinger, D. Kot, A. Huber, R. Kretschmer, T. Müller, A. Sattler, *ECS J. Solid State Sci. Technol.* **2020**, 9, 064002.
- [36] S. Rein, S. Diez, R. Falster, S. W. Glunz, in *Proc. 3rd World Conf. Photovoltaic Energy Conversion*, Osaka **2003**, p. 1048.
- [37] R. Swaroop, N. Kim, W. Lin, M. Bullis, L. Shive, A. Rice, E. Castel, M. Christ, *Solid State Technol.* **1987**, 3, 85.
- [38] Semiconductor Equipment and Materials International (SEMI), SEMI MF1239 **2021**.
- [39] M. Hourai, T. Nagashima, E. Kajita, S. Miki, T. Shigematsu, M. Okui, *J. Electrochem. Soc.* **1995**, 142, 3193.
- [40] M. Hourai, T. Nagashima, H. Nishikawa, W. Sugimura, T. Ono, S. Umeno, *Phys. Status Solidi A* **2019**, 216, 1800664.
- [41] V. V. Voronkov, *J. Cryst. Growth* **1982**, 59, 625.
- [42] J. Vanhellemont, *J. Appl. Phys.* **2011**, 110, 063519.
- [43] D. Walter, B. Lim, K. Bothe, R. Falster, V. Voronkov, J. Schmidt, in *27th European Photovoltaic Solar Energy Conf.*, WIP Munich, Frankfurt, Germany **2012**, p. 775.
- [44] R. Falster, V. Voronkov, V. Resnik, M. Milvidskii, *Electrochem. Soc. Proc.* **2004**, 2004–05, 188.
- [45] G. Kissinger, T. Müller, A. Sattler, W. Häckl, P. Krottenthaler, T. Grabolla, H. Richter, W. von Ammon, *Mater. Sci. Semicond. Process.* **2006**, 9, 236.
- [46] D. Kot, G. Kissinger, M. A. Schubert, S. Marschmeyer, G. Schwalb, A. Sattler, *Phys. Status Solidi C* **2017**, 14, 1700161.
- [47] G. Kissinger, J. Vanhellemont, U. Lambert, D. Gräf, H. Richter, *Microelectron. Eng.* **1999**, 45, 155.
- [48] Vienna Ab Initio Simulation Package, <https://www.vasp.at> (accessed: June 2021).
- [49] K. Momma, F. Izumi, *J. Appl. Crystallogr.* **2011**, 44, 1272.
- [50] K. Lauer, S. Krischok, T. Klein, M. Bähr, A. Lawrenz, R. Röder, T. Ortlepp, U. Gohs, *Phys. Status Solidi A* **2019**, 216, 1900284.
- [51] L. C. Kimerling, M. T. Asom, J. L. Benton, P. J. Drevinsky, C. E. Cafer, *Mater. Sci. Forum* **1989**, 38–41, 141.
- [52] E. Tarnow, *Europhys. Lett.* **1991**, 16, 449.
- [53] J. Zhu, T. D. Dela Rubia, L. H. Yang, C. Mailhot, G. H. Gilmer, *Phys. Rev. B* **1996**, 54, 4741.
- [54] B. Sadigh, T. J. Lenosky, S. K. Theiss, M.-J. Caturla, T. D. de la Rubia, M. A. Foad, *Phys. Rev. Lett.* **1999**, 83, 4341.
- [55] W. Windl, M. M. Bunea, R. Stumpf, S. T. Dunham, M. P. Masquelier, *Phys. Rev. Lett.* **1999**, 83, 4345.
- [56] P. Alippi, L. Colombo, P. Ruggerone, A. Sieck, G. Seifert, T. Frauenheim, *Phys. Rev. B* **2001**, 64, 075207.
- [57] J. Troxell, G. Watkins, *Phys. Rev. B* **1980**, 22, 921.
- [58] R. Harris, J. Newton, G. Watkins, *Phys. Rev. Lett.* **1982**, 48, 1271.
- [59] R. D. Harris, G. D. Watkins, L. C. Kimerling, *Mater. Sci. Forum* **1986**, 10–12, 163.
- [60] A. K. Tipping, R. C. Newman, *Semicond. Sci. Technol.* **1987**, 2, 389.
- [61] G. Fladda, K. Björkqvist, L. Eriksson, D. Sigurd, *Appl. Phys. Lett.* **1970**, 16, 313.
- [62] J. C. North, W. M. Gibson, *Appl. Phys. Lett.* **1970**, 16, 126.
- [63] W. Seelinger, B. Fischer, E. Diehl, K.-H. Ergezinger, H.-P. Frank, B. Ittermann, F. Mai, G. Welker, H. Ackermann, H. J. Stöckmann, *Nucl. Instrum. Methods Phys. Res., Sect. B* **1992**, 63, 173.
- [64] H. Metzner, G. Sulzer, W. Seelinger, B. Ittermann, H.-P. Frank, B. Fischer, K.-H. Ergezinger, R. Dippel, E. Diehl, H.-J. Stöckmann, *Phys. Rev. B* **1990**, 42, 11419.
- [65] E. Napolitani, D. De Salvador, R. Storti, A. Carnera, S. Mirabella, F. Priolo, *Phys. Rev. Lett.* **2004**, 93, 055901.
- [66] T. Schutz-Kuchly, J. Veirman, S. Dubois, D. R. Heslinga, *Appl. Phys. Lett.* **2010**, 96, 093505.
- [67] L. Vines, E. V. Monakhov, A. Y. Kuznetsov, R. Kozłowski, P. Kaminski, B. G. Svensson, *Phys. Rev. B* **2008**, 78, 085205.
- [68] J. Cardenas, B. G. Svensson, W.-X. Ni, K. B. Joelsson, G. V. Hansson, *Appl. Phys. Lett.* **1998**, 73, 3088.
- [69] S. Mirabella, D. De Salvador, E. Napolitani, E. Bruno, F. Priolo, *J. Appl. Phys.* **2013**, 113, 031101.
- [70] M. Moll, in *Proc. 28th Inter. Workshop on Vertex Detectors — PoS(Vertex2019)*, Sissa Medialab, Lopud, Croatia **2020**, p. 027.
- [71] D. Sheppard, R. Terrell, G. Henkelman, *J. Chem. Phys.* **2008**, 128, 134106.



**Kevin Lauer** studied technical physics and physics at Technical University of Ilmenau and Friedrich Schiller University Jena. In 2005, he received his diploma. Since 2005, he has been at the CiS research institute for micro systems technology. He received his Ph.D. in 2009 on applied physics. Since 2018, he has been partly employed at the Technical University of Ilmenau. His research fields are measurement method development, defects and defect engineering in silicon and silicon devices, development of microsensors such as pressure sensors, and photo and radiation detectors like low-gain avalanche diodes.



**Katharina Peh** obtained a training as a pharmaceutical technical assistant in Würzburg and Fulda and then she studied energy and environmental systems engineering in Ansbach and graduated with a bachelor of engineering. She then completed her master's program in regenerative energy technology with a focus on photovoltaics in Ilmenau and graduated with a master of science degree and worked as a process engineer in semiconductor laser production in Meiningen. She currently works as a research assistant in the Department of Technical Physics at the TU Ilmenau.



**Dirk Schulze** studied physics and technology of electronic components at the Technical University of Ilmenau and received his Ph.D. in 1990 in theoretical physics. After his doctorate, he worked as a research assistant at the Technical University of Ilmenau, at the Institute of Physics, and at the Institute of Economics in projects concerning the use of solar energy. After his employment at PV Silicon GmbH Erfurt as development manager, he became in 2000 development engineer for teaching and research at the Technical University of Ilmenau, leads the lecture collection for experimental physics, and researches and teaches in the field of photovoltaics.



**Thomas Ortlepp** studied mathematics at the Technical University of Ilmenau. He received his Ph.D. in quantum electronics in 2004. In 2010, he habilitated in the field of microelectronics and subsequently took over the leadership of an industrial project for high-performance quantum memory circuits at the University of Berkeley in California. In 2015, he was appointed distinguished professor at Yokohama National University. Also, in 2015, he took over the management of the CiS Forschungsinstitut für Mikrosensorik until today. His research focuses on development of silicon microsystems (MEMS and MOEMS) and the industrial application of quantum technology.



**Erich Runge** studied in Frankfurt/Main and received his Ph.D. from the TU Darmstadt with a thesis written at the Max-Planck-Institute FKF in Stuttgart. His path led him via Harvard University, HU Berlin, and MPI PKS in Dresden to the Technische Universität Ilmenau. There, he heads the department "Theoretical Physics I." He has about 150 papers on subjects ranging from ultrafast nanooptics over density functional theory and computational physics to photovoltaics and the physics of frustrated or disordered systems were cited more than 10 000 times (ResearchGate).



**Stefan Krischok** studied physics at the Clausthal University of Technology (Germany) from 1991 to 1997 and graduated there in 1997 with a diploma in physics. He got his Dr. rer. nat. (Ph.D.) in 2001 at the same university. During his Ph.D., he spent 1 year at Texas A&M university. In 2002, he moved to Technische Universität Ilmenau (Germany) where he got his habilitation for experimental physics in 2007. After leading an independent research group, he became the head of the group "Technical Physics" in 2014. His interests are in the field of surface and interface science.